



An apparatus for producing tunable, repeatable, hydrogen–oxygen-deflagrative blast waves

T. Skinner¹ · M. J. Hargather² · J. Blackwood¹ · M. Hays¹ · M. Bangham³

Received: 22 October 2018 / Revised: 15 August 2019 / Accepted: 27 August 2019
© Springer-Verlag GmbH Germany, part of Springer Nature 2019

Abstract

The Hydrogen Unconfined Combustion Test Apparatus (HUCTA) was designed and built to study the blast waves produced from unconfined hydrogen/oxygen deflagrations. The HUCTA uses evacuated balloons of up to 2 m in diameter which are filled with a combustible combination of gaseous hydrogen–oxygen mixtures. The well-mixed gases are ignited with an electric spark at the center of the sphere, resulting in a gaseous deflagration propagating through the mixture and a shock wave produced in the air. The combinations of balloon size and fuel/oxidizer ratios allow for a wide range of blast waves to be produced. Overpressures are measured with standard blast gauges at a variety of locations, demonstrating a high degree of radial symmetry and repeatability in the shock wave pressures, as well as the ability to produce non-ideal shock wave pressure profiles under some conditions. The range of peak pressures and explosive impulses obtainable is described as a function of mixture ratio. High-speed retroreflective shadowgraphy is used to visualize shock wave propagation and coalescence in individual frames and digital streak images. Since HUCTA is elevated approximately 2 m off the ground, there is a significant area around the apparatus where non-noisy, un-reflected, symmetric blast waves propagate; this area is ideal for testing items whose response to blast waves is desired for safety considerations.

Keywords Shadowgraph · Blast loading · Gas explosion

1 Introduction

Assessing blast effects on equipment is critical for scenarios where the equipment must function properly under explo-

Communicated by D. Frost and A. Higgins.

✉ M. J. Hargather
michael.hargather@nmt.edu

T. Skinner
troy.skinner@nasa.gov

J. Blackwood
james.m.blackwood@nasa.gov

M. Hays
michael.j.hays@nasa.gov

M. Bangham
mike.bangham@banghamengineering.com

¹ Jacobs Space Exploration Group, 620 Discovery Drive, Building 2, Suite 140, Huntsville, AL 35806, USA

² New Mexico Institute of Mining and Technology, 801 Leroy Place, Socorro, NM 87801, USA

³ Bangham Engineering, Inc., 1300 Meridian St., Suite 11, PO Box 4978, Huntsville, AL 35801, USA

sive loading in order to ensure the survival of personnel, including chemical plants, the oil and gas industry, military operations, spaceflight operations, and emerging industries such as hydrogen fuel cell automobiles. Limited methods exist for producing repeatable and tunable blast loading for statistical and parametric assessment of loading scenarios.

One traditional approach to controlled blast testing utilizes shock tubes to produce shock waves of known impulse and peak pressure [1]. While shock tubes have specific advantages such as being tunable, repeatable, and operated with rapid turnaround, the blast impulses are not always directly equivalent to a free-air explosion. The pressure-time profile in shock tubes can be tailored by changing the driver length, pressure, gas type, and end-wall configuration given sufficient facility flexibility [2]. A semi-analytical method to predict the pressure evolution in shock tubes has recently been published [3]. Test articles for shock tubes must fit within the tube or be placed near the exit of the tube which experiences a complex fluid dynamic loading due to the vortex ring produced [4].

Testing can be performed using high explosives directly to apply dynamic loading. This has been used to characterize

equipment response to varied loadings [5,6], but can be time-consuming and expensive to evaluate a wide range of loading scenarios.

The use of gaseous deflagrations and detonations to produce shock waves has been previously summarized and reviewed by Leyer et al. [7]. This review summarized testing with shock pressures less than 60 kPa and included a theoretical model for the flame front propagation and pressure field. Field tests with 1.5-m latex balloons filled with hydrogen and air were performed by Otsuka et al. [8] demonstrating variable pressure profiles with varied stoichiometries and distances. Methods for measuring the flame front from high-speed digital images were presented. The resulting pressure profiles had peak pressures less than 15 kPa and did not achieve true shock wave profiles. Kim et al. developed multiple test apparatuses and techniques for observing flame speed and acceleration of blast waves ranging in size from small soap bubbles to a 27-m³ tent for large-scale hydrogen–air testing [9–11]. The small-scale tests were done in an environment that provided for the use of schlieren techniques to observe combustion cell properties, flame acceleration, and differentiation of the different zones of interest. The large-scale tests utilized a cubic tent to study flame speed and gather blast overpressure from an unconfined explosion, which resulted in a simple model for flame acceleration useful for explosion sizes exceeding 1 m. These collected works also found that the flame propagation behaviors for the stoichiometric mixtures were similar to each other and that velocity increased continuously during the flame propagation. Pressure-time histories showed a continuous rise in pressure in the atmosphere in the near field, which transitioned to a shock wave and then at long distances decayed to a gradual pressure rise.

Larger-scale field tests with cylindrical and rectangular tents filled with hydrogen–air mixtures to produce blast waves have been performed by Wakabayashi et al. [12,13]. These tests included stoichiometric hydrogen–air mixtures performed at three different volumes with a rectangular tent [13] and three different concentrations performed in a cylindrical setup [12]. The resulting scaled overpressures were smaller than those expected by TNT equivalence methods; however, the scaled impulse observed was of the order expected. Composition C-4 explosive was used to initiate the mixture at the center of the tent, which introduces costs and safety considerations similar to direct explosive testing. The testing showed that the amplitude of the overpressure is dependent on the concentration of hydrogen and that the overpressure is increased by an order of magnitude when using high explosives as an initiator [12].

The majority of the previously published work on gas deflagration explosions has developed pressure pulses with less than 60 kPa peak pressure. The work presented here demonstrates the ability to produce larger pressure pulses,

including blast-like shock wave pressure profiles, with varied pressure impulses. High-speed retroreflective shadowgraphy allows visualization of the shock wave coalescence and propagation. The explosion process is also studied with digital streak imaging, allowing measurement of flame and shock velocities.

2 Design of HUCTA and characteristics

The Hydrogen Unconfined Combustion Test Apparatus (HUCTA) is an engineering system used to fill and ignite gaseous mixtures at varied stoichiometries to produce tunable blast waves for experimental testing. The HUCTA was originally designed to study the blast waves produced from unconfined hydrogen/oxygen deflagrations [14]. As presented here, the system is capable of producing a range of explosively driven shock and pressure wave flows which can be used to evaluate equipment response to explosive loading. The design of the system allows rapid turnaround, with up to 20 tests conducted in a day.

HUCTA is composed of four sub-systems: filling, mixing, ignition, and measurement. The first three sub-systems are shown schematically in Fig. 1a, and the full system in operation is shown in Fig. 1b with the blast pressure probes surrounding the explosion. The filling sub-system starts with compressed tanks of fuel and oxidizer. The gases are piped through stainless steel hoses to explosion-proof fill valves located just under the spherical balloon. These fill valves are actuated by a remote operator. In the event of power loss or pneumatic pressure loss, these valves automatically vent the gas mixture from the system. The mixing systems consist of two explosion-proof valves, an explosion-proof pump, and a gas sensor. The pump performs several duties. First, it evacuates the balloon so that no air is present at the time of filling to ensure that the ignited mixture contains no contaminants. Second, it keeps the gas recirculating within the balloon so the gases stay well mixed and do not stratify. Third, it diverts some of the gas through an explosion-proof container which houses gas sensors which include hydrogen, methane, and oxygen sensors here, but can be changed for other fuels. The mixture sensor provides a current measurement of the concentration inside the balloon which is monitored before a test. The pump and valve system also allows for deflating the balloon, removing a set quantity of gas, or adding air to the system.

Balloons are attached to the top of the HUCTA at the end of the fill system. Spherical balloons of up to 2 m diameter have been used, but the present testing uses 0.5-m-diameter polyethylene bags as near-transparent balloons to allow internal shadowgraph imaging.

The apparatus uses a gas delivery system to fill the balloons with combustible mixtures which can be tuned in

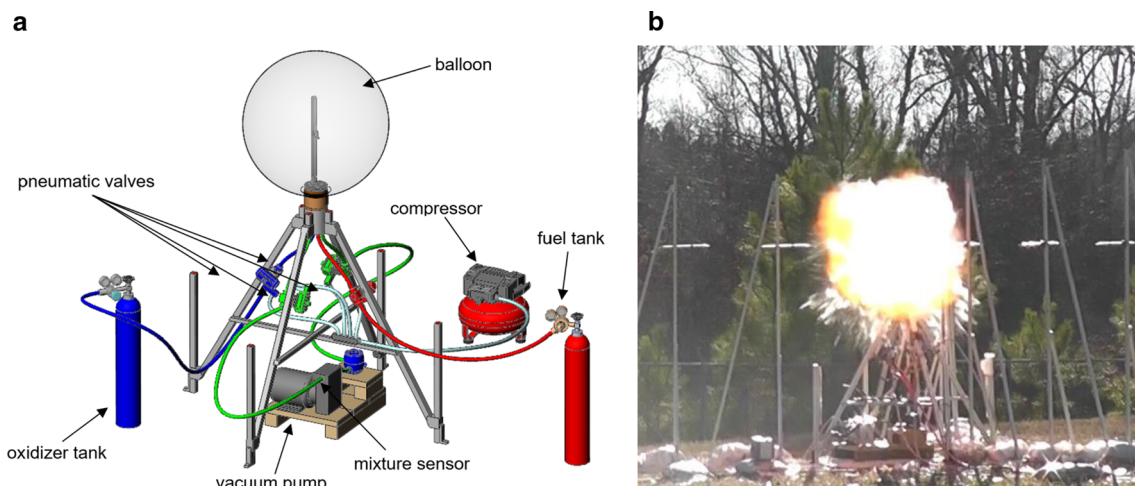


Fig. 1 The Hydrogen Unconfined Combustion Test Apparatus (HUCTA) shown **a** schematically and **b** during testing

stoichiometry. Once filled, the well-mixed gases are ignited with an electric spark at the center of the sphere. The ignition system is a simple electric coil spark ignitor that is remotely activated by the operator. It is a modular system which can be moved vertically so it is at the center of any size balloon, and it could easily be replaced by a different device such as an electric match or blasting cap if required. Significant work has been performed by other researchers on the ignition of gaseous mixtures, which has been reviewed recently by Kundu et al. [15]. The ignition here was repeatable, and studies of ignition energy variations are outside of the present scope.

The design of HUCTA places the bottom of the balloons at approximately 2 m off the ground. This provides a significant distance and space in which to conduct tests before ground reflections occur. The length of test time before the arrival of reflections varies with the shock wave speed, stoichiometry, and distance from the balloon but can be estimated from a given test shock velocity. In general, the geometry allows for at least 10 ms of test time before reflections arrive. Test articles can be placed almost anywhere around HUCTA to provide different shock wave characteristics and shapes. Spherical or cylindrical waves are generated near the balloon depending on the chosen balloon shape, which has been described previously by other researchers [16]. In the far field, these blast waves are still spherical, but the radius is large enough to approximate a planar wave for all but the largest of test samples.

3 Data acquisition

The measurement system consists of PCB piezoelectric blast probes (Model Number 137B23B, observable in Fig. 1b as elevated horizontal probes pointing at center of blast), a signal conditioner, and a National Instruments data acquisition

system. The blast gauge measurements are located in-plane and in-line with the center of ignition within the sphere. Additionally, they are attached to low-resonant-frequency stands to ensure no false noise is introduced into the sensor from structural vibration. Typically, blast sensors are arranged in three radials separated by 120°, between 0 and 10 m from the center of explosion; however, the sensors are portable and can be easily moved to a variety of locations. A peak acquisition rate of 500 kHz per sensor is possible.

Explosion phenomena are recorded with a variety of high-speed cameras (various Photron and Phantom models, both monochrome and color) typically operating around 10,000 frames per second (fps), but speeds of up to 180,000 fps have been used. Two cameras are used simultaneously, with one tightly focused on the initial blast for flame front velocity calculations and the other providing a wide-angle view to visualize shock propagation. Various filters are used on the cameras depending on what phenomena are being measured, such as flame speed or shock wave shadowgraphy. The balloon and any wiring or insulation tend to burn strongly in the infrared (IR) spectrum, so an IR filter significantly reduces the direct illumination that obscures the primary flame propagation of the mixed gases. Even though the primary combustion event emits light mostly in the ultraviolet (UV) spectrum, all cameras used thus far have sufficient sensitivity in the UV-A spectrum to easily resolve the flame front. Camera initiation is started by a TTL signal sent by the data acquisition at the time of spark coil initiation. All graphs presented here have time zero at the moment of spark coil ignition.

Retroreflective shadowgraphy is used to visualize shock wave and product gas motions. The retroreflective shadowgraph technique uses a 1000-W arc lamp (Newport Oriol), which is focused to a point onto a rod mirror mounted in front of and centered on the camera lens [17,18]. The light is thus redirected and projected to a retroreflective screen.

Fig. 2 **a** Image of the test setup showing the shadowgraph system and HUCTA with an un-inflated balloon installed. **b** Shadowgraph image from a typical test showing the shock wave, product gases, and failing balloon surface



The HUCTA is positioned between the camera and screen, approximately 5 m from the screen and 15 m from the camera. A high-speed digital video camera is used to record the shadowgraph images. Figure 2 shows an image of the shadowgraph setup and a typical shadowgram from testing.

4 Shadowgraph imaging of explosion process

The explosion process is imaged here using shadowgraphy to visualize shock wave and product gas motions. Figure 3 is a set of images from a single experiment recorded at 10,000 fps. The test was of a 0.5-m-diameter polyethylene bag filled with 67% hydrogen and 33% oxygen by volume. The first image is immediately before the ignitor is initiated and shows a typical pretest image. The primary source of error between tests is the position of the balloon immediately before ignition, which can be seen in this first frame to be slightly off center. The testing is conducted outdoors, and this particular test shows the effect of ambient wind, which caused the balloon to oscillate slightly on the HUCTA. The test was initiated during a calm point, but the balloon is seen to be leaning to the left. Future work is exploring methods to anchor the balloon internally to limit any effects of wind, but all data recorded here were with ambient wind oscillations and the data still show good symmetry as discussed below. The individual images show the growth of the flame front, which eventually ruptures the balloon, releasing a shock wave and late-time turbulent mixing of the combustion gases with the environment. The balloons fracture into many small pieces which are generally consumed in the fireball.

To better study the explosion process, streak images are created from the high-speed video frames. This technique, which is increasingly used to study transient flows [18,19], extracts a single pixel row from each high-speed image and vertically concatenates the rows to create a digital streak image with time increasing in the downward direction. The

streak image shown in Fig. 4 was created from a test performed with the same 67% hydrogen and 33% oxygen by volume mixture, recorded at 180,257 fps, with a single row extracted from 1600 individual frames. The vertical time is therefore 8.88 ms, and the horizontal length is approximately 2.2 m. The image in Fig. 4a is from the raw frames, and Fig. 4b has been image-processed by performing a background subtraction of the initial frame to highlight differences between images and better reveal the shock wave. The streak image shows the expansion of the flame front inside the balloon and resulting shock wave propagation. The image shows that the balloon surface begins expanding as the combustion propagates within and ultimately fractures at several locations. A single shock wave is produced with some weak, near sonic waves, emanating after the initial shock wave. The velocity of the flame front and shock waves can be measured from the slope on the streak diagram. The flame front is observed to propagate here at a constant 105 ± 10 m/s. The shock wave velocity is initially 450 ± 10 m/s as it emerges from the balloon surface and decays to 400 ± 10 m/s by the edge of the streak image frame shown here.

The streak imaging technique is used here to study the shock wave formation and coalescence for different mixture ratios. The difficulty in the streak measurements is that high-time-resolution video sequences are needed for clear streak images to be produced, but most testing uses wider fields of view and lower time resolutions to visualize large-scale propagation. Note that streak images can be created from low-time-resolution image sequences, like those in Fig. 3, and the same analysis performed to extract velocities of features. For the image sequence in Fig. 3, a streak image created was analyzed to measure a flame front velocity of 102 ± 15 m/s, which is the same as measured from Fig. 4 to within experimental uncertainties. Lower time resolution in streak images results in step-like increments of feature motions, which can add uncertainty to velocity measurements as reported here.

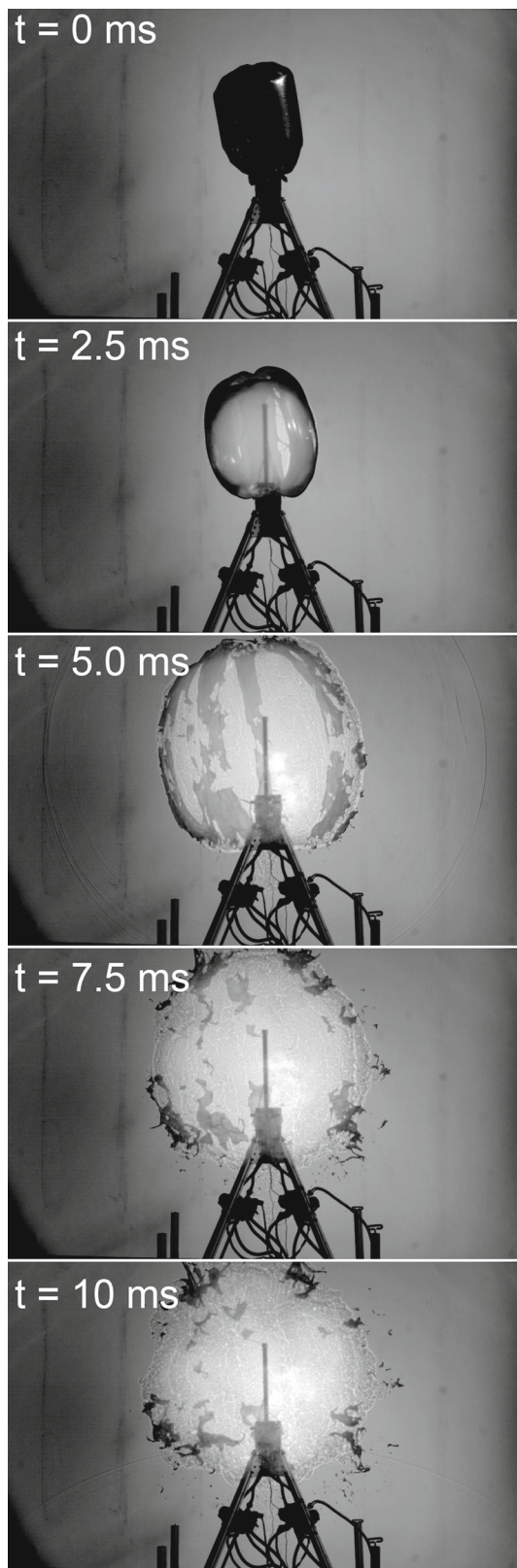


Fig. 3 Image sequence from an individual test with 67% H₂ and 33% O₂ by volume. The field of view is approximately 3.0 m wide. The individual images are recorded using a Phantom v1610, at 10,000-fps and 0.45- μ s exposure. The first frame is immediately before ignitor initiation, and the shock wave is visible in the frame $t = 5$ ms

5 Tunable shock wave characteristics

Varying combinations of balloon size, fuel, oxidizer, and stoichiometry allow for a wide range of blast waves to be produced with HUCTA. The combustible gas region can be tailored by the balloon attached to produce cylindrical or spherical symmetry. When spherical balloons are used and ignited in the center, the blast waves are radially symmetric in all directions. For cylindrical balloons, as shown in Fig. 2, the blast waves are radially symmetric but can vary vertically. In either geometry case, different locations around HUCTA at the same height and radial distance produce highly similar shock wave profiles. Figure 5 shows three (unfiltered) pressure traces from a single test with a spherical balloon with a diameter of 1.5 m containing 70.4% hydrogen and 29.6% oxygen. Each sensor was placed at the same distance from the center of explosion, but separated by 120° around the circumference of the balloon. These pressure traces are essentially the same, supporting the symmetry of the explosion. Other reported fuel–oxidizer test platforms have shown comparable pressure symmetry [8] or slightly reduced symmetry [20,21], and some apply filtering to remove noise [22]. The symmetry of the blast field around HUCTA allows multiple blast wave interaction tests to be conducted simultaneously along different radials.

The pressure measurements show that a shock wave is produced for this test condition at all of the distances measured. The pressure trace at the 1.5-m location (gages 1, 4, and 7) shows two shock pulses, indicating that the shock wave may not be fully coalesced. Similar pressure traces have been observed by others in vapor cloud explosions [23] and coalescing low-grade detonations of propellants [24]. The second shock pulse is observed to be of the same or greater peak pressure than the primary shock wave because it is traveling through the shocked atmosphere at a velocity faster than the leading shock wave, resulting in a larger pressure increase. The high-speed shadowgraph imaging was not able to determine any definitive source of this strong secondary wave. Using the time of arrival of the secondary shock wave and analysis of the streak image in Fig. 4, it is hypothesized that the wave is a secondary shock wave formed from the reflected expansion of the gases at the moment the balloon surface first ruptures. Courtaud et al. [25] present an excellent streak wave diagram of an explosion process and the formation of the secondary shock wave from the reflected expansion wave which is hypothesized here. In some studies, the confining balloon surface is ruptured immediately before a test to reduce this effect [7,8].

Figure 6 shows pressure profiles from two specific sensor locations, but from two different tests conducted on different days. This figure details the repeatability of the testing. The red curve is from a test with a 1.4-m-diameter balloon with 67.4% hydrogen and 32.6% oxygen by volume. The

Fig. 4 Digital streak images created from individual high-speed video frames using **a** raw images and **b** image-processed frames to enhance visibility of shock wave propagation. The vertical extent represents 8.88 ms, and the horizontal width is approximately 2.2 m

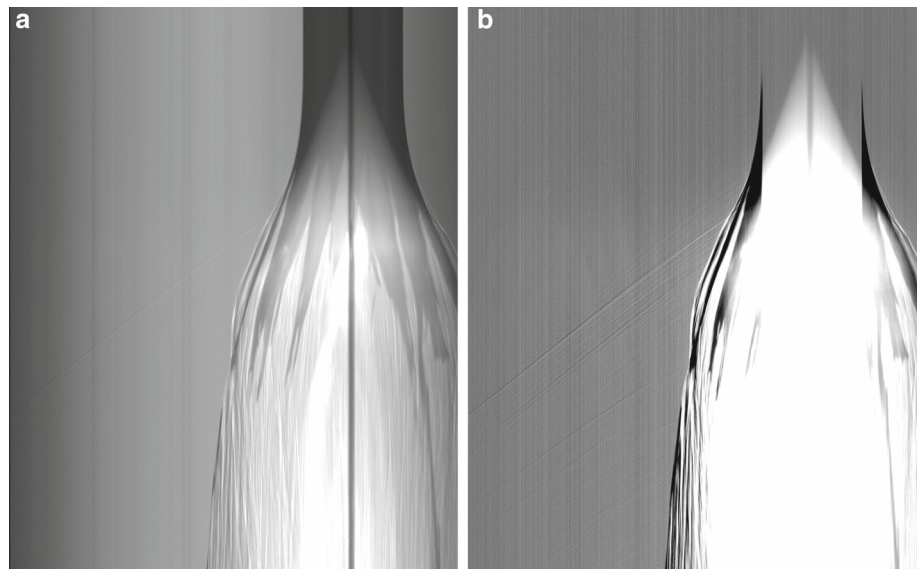
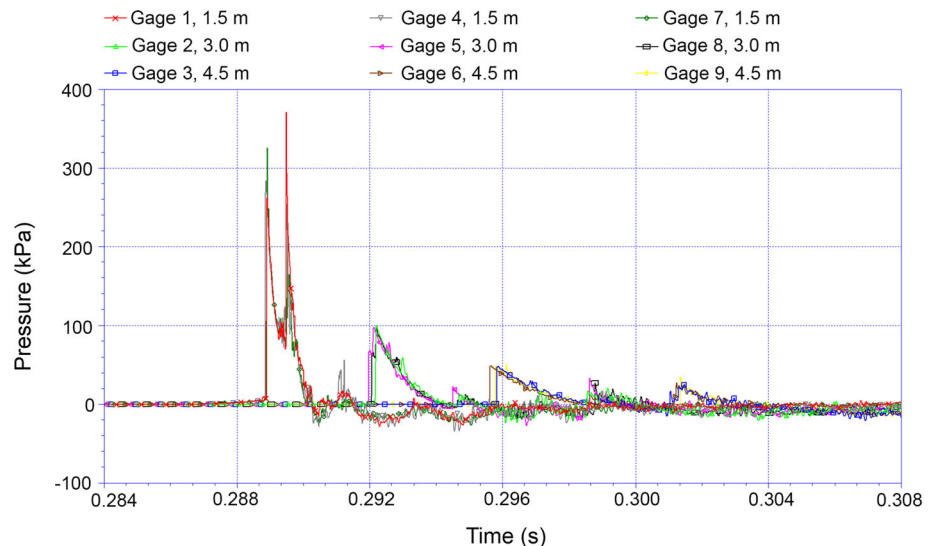


Fig. 5 Pressure traces at three different locations along three different radials during a single HUCTA test, showing high degree of blast symmetry. The radial distances are 1.5 m for gages 1, 4, and 7, 3.0 m for gages 2, 5, and 8, and 4.5 m for gages 3, 6, and 9



green curve is from a test with the same balloon diameter and a nearly identical 66.5% hydrogen and 33.5% oxygen mixture. Figure 6a shows two sensors located near the edge of the balloon. This is within the distance where the shock is still coalescing and shows a double-peak structure. Figure 6b shows the second set of sensors several feet away from the edge of the balloon in the fully developed shock region. The near-field region clearly does not produce a pressure-pulse equivalent to an explosively formed shock wave, but the far-field region does. The location of this transition varies for different mixture ratios and gas species. Regardless of the delineation of the near versus far field, these data show good repeatability of pressure pulses in all regions. The variation of approximately 1% hydrogen content also is not observed to have an appreciable change in the pressure profiles as recorded.

The blast wave profiles can also be tuned to particular impulses and peak overpressures by varying the mixture ratios. Figure 7 shows the variation in impulse and peak overpressure at a single location as a function of mixture ratio. Each data point in Fig. 7 is an average from at least three tests with the 0.5-m-diameter balloons, measured at a distance of 1.07 m from the ignition point. Typically, impulse and overpressure variations of less than 15% are seen between tests of the same mixture ratio. Some of this error can be attributed to differences in atmospheric conditions between tests, which could be corrected for using Sachs scaling [26], but is not applied here.

Ideal explosives usually form a classic shock wave as shown in the HUCTA overpressure data of Fig. 5. This type of blast wave is generally produced when the combustible mixture of hydrogen and oxygen is at or near stoichiometric. However, it is possible to generate other forms of blast

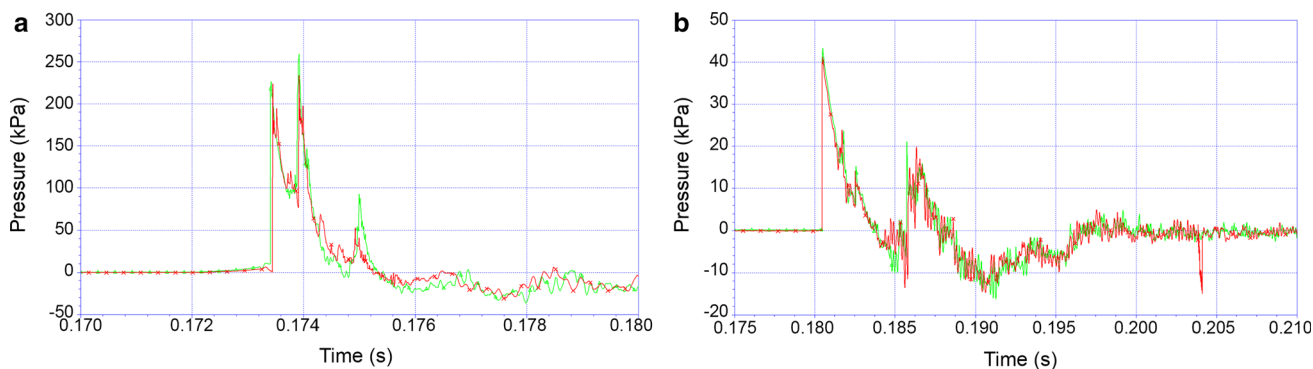
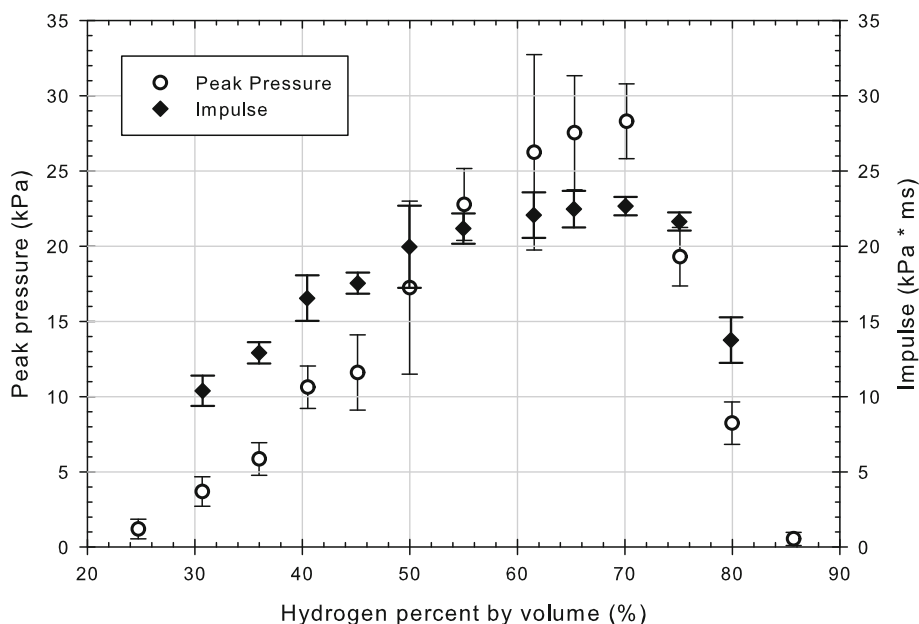


Fig. 6 Pressure traces from two different tests with approximately the same balloon gas content, measured with the same sensors positioned at **a** 1.5 m where two shock waves are observed and at **b** 3 m where a single coalesced shock is observed

Fig. 7 Impulse and peak overpressure variation as a function of mixture ratio at 1.07 m from the ignition of the 0.5-m-diameter balloons



waves. For example, Fig. 8 shows a variety of non-shocked triangular blast waves followed by a non-triangular negative phase with a slight positive rebound. This type of blast wave is often generated by non-ideal explosives [27]. These non-ideal explosive waveforms are characterized by lower peak overpressures and longer rise times than ideal explosions. Testing under these types of non-shocked blast waves is gaining interests as the prevalence of non-high explosive (non-HE) improvised explosive devices (IEDs) increases.

6 Applications and future work

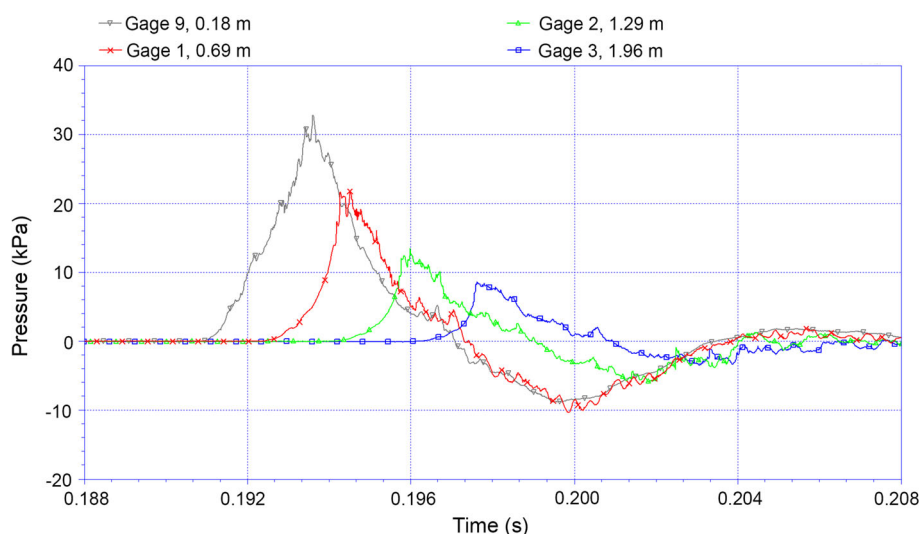
Some of the current and potential applications of HUCTA include:

1. Distant focused overpressure (DFO): Explosions or noise generation of large magnitudes can reflect and be focused

by the atmosphere in such a way that window breakage and other damage can occur at distances far from the source. HUCTA is currently being considered as a device to better understand what overpressure/impulse combinations will break various types of windows.

2. Non-high explosive events: Since HUCTA can produce blast waves similar to those generated by non-ideal explosives, it can be used to quantify the damage to structures and personnel from these types of explosive events. Since HUCTA purposefully does not produce fragments or smoke, it is ideal for visualizing the blast effects on various objects.
3. Duplicate/model high-pressure tank explosions: HUCTA essentially produces a sphere of high-pressure gas that then accelerates and shocks up in the ambient atmosphere. Due to this fact, it approximates the blast waves generated by pressure tank ruptures. HUCTA can be used to produce this type of blast wave without the addition of

Fig. 8 Non-ideal triangular pressure waves produced by HUCTA with a 0.5-m-diameter polyethylene balloon with 65.5% hydrogen and 34.5% oxygen. The pressure gages 9, 1, 2, and 3 are at radial distances of 0.18 m, 0.69 m, 1.29 m, and 1.96 m, respectively



high-speed fragments that an actual pressure tank rupture would produce.

- Determine blast wave produced by various explosive gas mixtures: HUCTA has been used thus far to study the blast waves produced from hydrogen/air, hydrogen/oxygen, methane/air, and methane/oxygen. Many other fuel and oxidizer combinations could be tested such as propane, acetylene, particulates, and nitrous oxide. Inert gases such as carbon dioxide, helium, or argon could be inserted to determine their effect on reducing the blast wave strength.

7 Conclusions

The Hydrogen Unconfined Combustion Test Apparatus (HUCTA) was designed to study the combustion characteristics of freely expanding hydrogen/oxygen explosions including flame propagation within the combustible mixture and blast wave propagation in the surrounding air. Peak overpressures up to 340 kPa (50 psi) have been demonstrated. The classic shock wave is generated with near-stoichiometric mixtures of hydrogen/oxygen while non-ideal blast waves are produced by modifying the mixture ratio. Peak overpressure and impulse for a given location are varied through changes in mixture volume and composition. A wide variety of fuel and oxidizer combinations can be tested on HUCTA with only minor changes to sensors and regulators. HUCTA provides a new scientific capability to the industry in that it successfully incorporates symmetry, repeatability, and tunability in the creation of blast waves.

Acknowledgements This work was performed under NASA Contract NMM12AA41C.

References

- Igra, O., Seiler, F. (eds.): *Experimental Methods of Shock Wave Research*. Springer, Berlin (2016). <https://doi.org/10.1007/978-3-319-23745-9>
- Chandra, N., Ganpule, S., Kleinschmit, N.N., Feng, R., Holmberg, A.D., Sundaramurthy, A., Selvan, V., Alai, A.: Evolution of blast wave profiles in simulated air blasts: experiment and computational modeling. *Shock Waves* **22**, 403–415 (2012). <https://doi.org/10.1007/s00193-012-0399-2>
- Tasissa, A.F., Hautefeuille, M., Fitek, J.H., Radovitzky, R.A.: On the formation of Friedlander waves in a compressed-gas-driven shock tube. *Proc. R. Soc. A Math. Phys. Eng. Sci.* **472**(2186), 20150611 (2016). <https://doi.org/10.1098/rspa.2015.0611>. ISSN 1364-5021
- Giannuzzi, P.M., Hargather, M.J., Doig, G.C.: Explosive-driven shock wave and vortex ring interaction with a propane flame. *Shock Waves* **26**, 851–857 (2016). <https://doi.org/10.1007/s00193-016-0627-2>
- Jacinto, A.C., Ambrosini, R.D., Danesi, R.F.: Experimental and computational analysis of plates under air blast loading. *Int. J. Impact Eng.* **25**(10), 927–947 (2001). [https://doi.org/10.1016/S0734-743X\(01\)00031-8](https://doi.org/10.1016/S0734-743X(01)00031-8)
- Aune, V., Fagerholt, E., Hauge, K.O., Langseth, M., Børvik, T.: Experimental study on the response of thin aluminium and steel plates subjected to airblast loading. *Int. J. Impact Eng.* **90**, 106–121 (2016). <https://doi.org/10.1016/j.ijimpeng.2015.11.017>. ISSN 0734-743X
- Leyer, J.C., Desbordes, D., Saint-Cloud, J.P., Lannoy, A.: Unconfined deflagrative explosion without turbulence: Experiment and model. *J. Hazard. Mater.* **34**(2), 123–150 (1993). [https://doi.org/10.1016/0304-3894\(93\)85002-V](https://doi.org/10.1016/0304-3894(93)85002-V). ISSN 0304-3894d
- Otsuka, T., Saitoh, H., Mizutani, T., Morimoto, K., Yoshikawa, N.: Hazard evaluation of hydrogen–air deflagration with flame propagation velocity measurement by image velocimetry using brightness subtraction. *J. Loss Prev. Process Ind.* **20**(4), 427–432 (2007). <https://doi.org/10.1016/j.jlp.2007.04.031>. ISSN 0950-4230
- Kim, D., Usuba, S., Watanabe, Y., Nario, T., Kakudate, Y.: Measurements of flame propagation velocities and blast wave pressures for methane/oxygen gas mixtures. *Sci. Technol. Energ. Mater.* **73**(1–2), 47–52 (2012)
- Kim, W.K., Mogi, T., Dobashi, R.: Fundamental study on accidental explosion behavior of hydrogen–air mixtures in an open space. *Int.*

- J. Hydrog. Energy **38**(19), 8024–8029 (2013). <https://doi.org/10.1016/j.ijhydene.2013.03.101>
11. Kim, W.K., Mogi, T., Kuwana, K., Dobashi, R.: Prediction model for self-similar propagation and blast wave generation of premixed flames. *Int. J. Hydrog. Energy* **40**(34), 11087–11092 (2015). <https://doi.org/10.1016/j.ijhydene.2015.06.123>
 12. Wakabayashi, K., Mogi, T., Kim, D., Abe, T., Ishikawa, K., Kuroda, E., Matsumaura, T., Nakayama, Y., Horiguchi, S., Oya, M., Fujiwara, S.: A field explosion test of hydrogen–air mixtures. Proceedings of the HySafe International Conference on Hydrogen Safety, Pisa, Italy (2005)
 13. Wakabayashi, K., Nakayama, Y., Mogi, T., Kim, D., Abe, T., Ishikawa, K., Kuroda, E., Matsumura, T., Horiguchi, S., Oya, M., Fujiwara, S.: Experimental study on blast wave generated by deflagration of hydrogen–air mixture up to 200 m³. *Sci. Technol. Energ. Mater.* **68**(1), 25–28 (2007)
 14. Richardson, E., Skinner, T., Blackwood, J., Hays, M., Bangham, M., Jackson, A.: An experimental study of unconfined hydrogen/oxygen and hydrogen/air explosions. 46th JANNAF Combustion Conference, Albuquerque, NM (2014)
 15. Kundu, S., Zanganeh, J., Moghtaderi, B.: A review on understanding explosions from methane–air mixture. *J. Loss Prev. Process Ind.* **40**, 507–523 (2016). <https://doi.org/10.1016/j.jlp.2016.02.004>
 16. Knock, C., Davies, N.: Blast waves from cylindrical charges. *Shock Waves* **23**, 337–343 (2013). <https://doi.org/10.1007/s00193-013-0438-7>
 17. Hargather, M.J., Settles, G.S.: Retroreflective shadowgraph technique for large-scale visualization. *Appl. Opt.* **48**, 4449–4457 (2009). <https://doi.org/10.1364/AO.48.004449>
 18. Settles, G.S., Hargather, M.J.: A review of recent developments in schlieren and shadowgraph techniques. *Meas. Sci. Technol.* **28**, 042001 (2017). <https://doi.org/10.1088/1361-6501/aa5748>
 19. Kleine, H.: Time-resolved visualization of transient compressible flows. 15th International Symposium on Flow Visualization, Minsk, Belarus (2012)
 20. Bunker, R., Eck, M., Taylor, J.W., Hancock, S.: Correlation of liquid propellants NASA headquarters RTOP. Technical Report WSTF-TR-0985-001-01-02, NASA White Sands Test Facility (2003)
 21. Groethe, M.A., Colton, J., Chiba, S., Sato, Y.: Hydrogen deflagrations at large scale. 15th World Hydrogen Energy Conference, Yokohama, Japan (2004)
 22. Merilo, E.G., Groethe, M.A.: Deflagration safety study of mixtures of hydrogen and natural gas in a semi-open space. International Conference on Hydrogen Safety, San Sebastián, Spain (2007)
 23. Heymes, F., Aprin, L., Slangen, P., Lauret, P., Lapebie, E., Osmont, A.: An experimental study on vapor cloud explosion of propane–oxygen stoichiometric mixture. *Chem. Eng. Trans.* **53**, 61–66 (2016). <https://doi.org/10.3303/CET1653011>
 24. Kandula, M., Freeman, R.: On the interaction and coalescence of spherical blast waves. *Shock Waves* **18**(1), 21–33 (2008). <https://doi.org/10.1007/s00193-008-0134-1>. ISSN 1432-2153
 25. Courtiaud, S., Lecysyn, N., Damamme, G., Poinot, T., Selle, L.: Analysis of mixing in high-explosive fireballs using small-scale pressurised spheres. *Shock Waves* **29**(2), 339–353 (2019). <https://doi.org/10.1007/s00193-018-0814-4>. ISSN 1432-2153
 26. Dewey, J.M.: Expanding spherical shocks (blast waves). In: Bendor, G., Igra, O., Elperin, E. (eds.) *Handbook of Shock Waves*, vol. 2, pp. 441–481. Academic Press, Cambridge (2001). <https://doi.org/10.1016/B978-012086430-0/50029-4>
 27. Pape, R., Mniszewski, K.R., Longinow, A.: Explosion phenomena and effects of explosions on structures. I. Phenomena and effects. *Pract. Period. Struct. Des. Constr.* **15**(2), 135–140 (2010). [https://doi.org/10.1061/\(ASCE\)SC.1943-5576.0000038](https://doi.org/10.1061/(ASCE)SC.1943-5576.0000038)

Publisher's Note Springer Nature remains neutral with regard to jurisdictional claims in published maps and institutional affiliations.